Ibn Al-Haitham Journal for Pure and Applied Sciences
Journal homepage: jih.uobaghdad.edu.iq
PISSN: 1609-4042, EISSN: 2521-3407
IHJPAS. 2024, 37(4)

Stability and Bifurcation Analysis of the Impact of Refuge on the Dissolved Oxygen-Plankton Interaction

Ahmed Ali[1,*], Shireen Jawad[2] and Fengde Chen[3]

[1,2]Department of Mathematics, College of Science, University of Baghdad, Baghdad, Iraq.
[3]College of Mathematics and Statistics, Fuzhou University, Fuzhou 350108, P.R. China.
*Corresponding Author.

Received: 21 May 2023 Accepted: 9 July 2023 Published: 20 October 2024
doi.org/10.30526/37.4.3505

Abstract

The suggested mathematical model for studying the effect of refuge on the dissolved oxygen in the plankton ecosystem is based on measurements of dissolved oxygen, phytoplankton, and zooplankton populations. The aim of this work is to find out the potential equilibrium and to investigate their behaviour. The study shows that there are three points of equilibrium. The feasibility requirements and stability conditions for all steady states are determined. Using the consumption of oxygen by zooplankton as a bifurcation parameter, we test for the presence of Hopf- bifurcation for the interior equilibrium. It is shown what conditions must be met for stable limit cycles. Finally, a numerical simulation is conducted to back up the analytical findings. It shows when the stability criteria are met, the solution of the proposed system constantly oscillates around the positive stable state. In addition, the solution exhibits limit cycle behaviour for small changes in certain parameters.

Keywords: Plankton interaction, Stability analysis, Bifurcation, Dissolved oxygen model.

1. Introduction

Much effort has been put into understanding dissolved oxygen dynamics better since they are such a crucial indicator of the health of marine ecosystems [1-3]. Most of the oxygen in the oceans comes from phytoplankton which also serves as the foundation of the marine food chain through their photosynthesis [4]. It's well knowledge that salinity, temperature, and nutrient availability all play significant roles in determining how much oxygen phytoplankton can create. Additionally, there is a considerable diurnal variation in oxygen generation by phytoplankton. Therefore, the link between phytoplankton and dissolved oxygen is crucial to the existence of organisms. Oxygen production fluctuations can have severe consequences for marine life. [5]. Since oxygen is used by living things for photosynthesis (during the day) and respiration (at night), the amount of oxygen in the water changes day and night. As a result, phytoplankton colonies can serve as reliable markers of ecological status. [6], [7]. Mondal, and his colleague, for instance, have studied how the coupled plankton-oxygen dynamics in the ocean are affected by a low oxygen production rate, which can result in oxygen depletion and species extinction [8].

Furthermore, the primary objective of the study of theoretical ecology is to identify the various dynamical mechanisms underlying interactions between prey and predator [9-11]. The relationship between phytoplankton and zooplankton is an example of a predator-prey interaction that reveals numerous aspects of marine ecology. Phytoplankton contributes substantially to aquatic ecosystems, including producing vast quantities of oxygen, managing natural resources and water quality, and establishing multiple food webs [12-14]. Plankton dynamics research is a fascinating field of study. Plankton constitutes the building elements of all aquatic food chains, with phytoplankton occupying the first trophic level [15]. Bagheli and Dhar examine the effect of dissolved oxygen on the presence of a planktonic population that interacts. They conclude that Hopf-bifurcation in the interior equilibrium is possible if the phytoplankton growth rate is selected as the bifurcation parameter [16].

The purpose of this research is to examine how the phytoplankton refuge affects the dynamics of the oxygen-plankton model. Some phytoplankton may evade their zooplankton prey by relocating to deeper water column layers. These sediments offer shelter from predators to the prey. Here is how the article is laid out: in Sec. 2, we built the structure of the proposed model. Sec. 3 explains the feasibility requirements and stability conditions for all steady states. The prevalence of Hopf bifurcations is also illustrated in Sec. 4. In Sec. 5. we undertake MATLAB-based numerical simulations to validate the analytical results.

2. Construction of the Model

Include Let $u(t)$ and $v(t)$ indicate the phytoplankton and zooplankton populations at the time t, respectively. We assume some phytoplankton populations are safe from zooplankton predation because they can conceal themselves in the ocean's floor-diverse sediments. These sediments offer refuge from predators to the hunted. $w(t)$ represents the dissolved oxygen concentration in the marine. Since phytoplankton do photosynthesis throughout the day, they also contribute to atmospheric oxygen production. Several additional factors, such as the respiration of marine organisms, the consumption of oxygen by phytoplankton at night, and the gradual drop in oxygen concentration brought about by chemical reactions in the water, all affect the rate at which oxygen is depleted. The following set of ordinary differential equations serves as the governing structure for the dynamical system of the system (1):

$$\begin{aligned}
\frac{du}{dt} &= \frac{ru}{(a_1 + w_0 - w)} - \alpha_1 u(1-m)v - \delta_1 u, \\
\frac{dv}{dt} &= \frac{\alpha_2 u(1-m)v}{(a_2 + w_0 - w)} - \delta_2 v, \\
\frac{dw}{dt} &= s(w_0 - w) + du - \gamma w - \gamma_1 uw - \gamma_2 vw,
\end{aligned} \tag{1}$$

with the initial conditions $u(0) \geq 0, v(0) \geq 0$ and $w(0) \geq 0$. In the first equation of the system (1), $\frac{ru}{(a_1+w_0-w)}$ represents the absorption of dissolved oxygen from phytoplankton with the growth rate r. The maximum growth rate of the phytoplankton population is r/a_1 at $w = w_0$. α_1 is the phytoplankton's capture rate by zooplankton. $m \in (0,1)$ is the proportion of protected phytoplankton. $(1-m)$ is the ratio of unprotected phytoplankton devoured by different zooplankton groups. α_2 is the conversion rate from phytoplankton to zooplankton. δ_1 and δ_2 are the phytoplankton and zooplankton's natural death rates. a_1 is the phytoplankton saturation constant. a_2 is the zooplankton saturation constant. w_0 is the constant concentration of dissolved

oxygen that comes from external sources. s is the replenishment rate of oxygen in marine. d is the amount of oxygen produced as a result of the process of photosynthesis carried out by phytoplankton. γ is the natural depletion rate of oxygen. γ_1 is the consumption of oxygen by phytoplankton during the night. γ_2 is the consumption of oxygen by zooplankton.

The equations of the system (1) are $C^1(R_+^3)$, where $R_+^3 = \{(u,v,w), u \geq 0, v \geq 0, \ w \geq 0\}$. Consequently, they are Lipschitz Ian [17]. Therefore, the system's (1) solution exists and is unique.

2. Existence of equilibria

System (1) has three non-negative steady states, namely

1. $z_1 = (0,0,\widehat{w})$, where $\widehat{w} = \frac{sw_0}{s+\gamma}$.
2. $z_2 = (\bar{u}, 0, \bar{w})$, where $\bar{u} = \frac{(s+\gamma)(a_1\delta_1 - r)}{d\delta_1 - \gamma_1(\delta_1(a_1+w_0)-r)}$ and $\bar{w} = a_1 + w_0 - \frac{r}{\delta_1}$, and. Clearly, $\bar{u}$ and $\bar{w}$ are positive if the following condition is satisfied:
$$r < min.\{a_1\delta_1, \delta_1(d - \gamma_1(a_1 + w_0))\}. \quad (2)$$
3. $z_3 = (u^*, v^*, w^*)$, where $u = \frac{\delta_2(a_2+w_0-w)}{(1-m)[\alpha_2 - a(a_2+w_0-w)]}, v = \frac{r}{\alpha_1(1-m)(a_1+w_0-w)} - \frac{\delta_1}{\alpha_1(1-m)}$, and w is the root of the following equation:

$$B_0w^3 + B_1w^2 + B_2w + B_3 = 0, \quad (3)$$

where,

$B_0 = a\alpha_1(1-m)(s+\gamma) > 0,$

$B_1 = \alpha_1 asw_0[2-(1-m)] + d\delta_2\alpha_1 - \alpha_1(s+\gamma)(\alpha_2 - aa_2) - \alpha_1 a\gamma[a_1(1-m) - 2w_0]$

$B_2 = \alpha_1 asw_0(1-m)(2a_1 + 3w_0) - \alpha_1 w_0(1-m)(s+\gamma)[\alpha_2 - aa_2] - d\delta_2\alpha_1 a_1 + \alpha_1(1 - m)(s+\gamma)[aa_1a_2 - \alpha_2 a_1 + aw_0^2] + \alpha_1 a\gamma w_0(1-m)(a_1+w_0)$

$B_3 = \alpha_1 sw_0(1-m)[\alpha_2 a_1 - aa_1a_2 - aa_1w_0 + \alpha_2 w_0 - a\alpha_2 w_0 - aw_0^2] + d\delta_2\alpha_1[a_1a_2 + a_1w_0 + a_2w_0 + w_0^2].$

Using Descartes's rule of sign [15], equation (3) has a unique positive root, say $w = w^*$, if one of the following sets conditions hold:

$$B_1 > 0 \text{ and } B_3 < 0, \quad (4)$$
$$B_2 < 0 \text{ and } B_3 < 0.$$

For $u^*$and $v^*$to be positive, the following two conditions must be satisfied:

$$\alpha_2 > a(a_2 + w_0 - w), \quad (5)$$
$$r > \delta_1(a_1 + w_0 - w).$$

3. Stability Analysis

The feature of the eigenvalues of the Jacobian matrix $J(u,v,w)$ at an equilibrium point is directly related to the behaviour of the system (1) near an equilibrium. The $J(u,v,w)$ at any point, say (u,v,w), can be written as:

$$J = \begin{bmatrix} \frac{r}{(a_1+w_0-w)} - \alpha_1 v(1-m) - \delta_1 & -\alpha_1 u(1-m) & \frac{ru}{(a_1+w_0-w)^2} \\ \frac{\alpha_2 v(1-m)}{(a_2+w_0-w)} & \frac{\alpha_2 u(1-m)}{(a_2+w_0-w)} - \delta_2 & \frac{\alpha_2 u(1-m)v}{(a_2+w_0-w)^2} \\ d - \gamma_1 w & -\gamma_2 w & -(s+\gamma+\gamma_1 u+\gamma_2 v) \end{bmatrix}$$

The local stability of system (1) around each equilibrium is:

1. The Jacobian matrix at $z_1 = (0,0,\widehat{w})$ is given as:

$$J(z_1) = \begin{bmatrix} \frac{r}{(a_1 + w_0 - \widehat{w})} - \delta_1 & 0 & 0 \\ 0 & -\delta_2 & 0 \\ d - \gamma_1 \widehat{w} & -\gamma_2 \widehat{w} & -s - \gamma \end{bmatrix}$$

Then, $J(z_1)$ has the eigenvalues $\lambda_{11} = \frac{r}{(a_1+w_0-\widehat{w})} - \delta_1$, $\lambda_{12} = -\delta_2 < 0$, and $\lambda_{13} = -s - \gamma$. $z_1$is a locally asymptotically stable point if and only if

$$r < \delta_1(a_1 + w_0 - \widehat{w}) \tag{6}$$

2. The Jacobian matrix at $z_2 = (\bar{u}, 0, \bar{w})$ is given as:

$$J(z_2) = \begin{bmatrix} \frac{r}{(a_1 + w_0 - \bar{w})} - \delta_1 & -\alpha_1 \bar{u}(1-m) & \frac{r\bar{u}}{(a_1 + w_0 - \bar{w})^2} \\ 0 & \frac{\alpha_2 \bar{u}(1-m)}{(a_2 + w_0 - \bar{w})} - \delta_2 & 0 \\ d - \gamma_1 \bar{w} & -\gamma_2 \bar{w} & -s - \gamma - \gamma_1 \bar{u} \end{bmatrix}$$

Then, $|J(z_2) - I\lambda| = 0$ gives:

$$\left(\frac{\alpha_2 \bar{u}(1-m)}{(a_2 + w_0 - \bar{w})} - \delta_2 - \lambda\right)\left[\lambda^2 - Tr\big(J(z_2)\big)\lambda + Det\big(J(z_2)\big)\right]$$

The eigenvalues of the above equation can be written as follows

$\lambda_{21} = \frac{\alpha_2 \bar{u}(1-m)}{(a_2+w_0-\bar{w})} - \delta_2$,

$Tr\big(J(z_2)\big) = \frac{r}{(a_1+w_0-\bar{w})} - \delta_1 - (s + \gamma + \gamma_1 \bar{u})$,

$Det\big(J(z_2)\big) = \delta_1(s + \gamma + \gamma_1 \bar{u}) + \frac{r\bar{u}\ (\gamma_1 \bar{w} - d)}{(a_1+w_0-\bar{w})^2} - \frac{r(s+\gamma+\gamma_1 \bar{u})}{(a_1+w_0-\bar{w})}$.

Clearly, z_2 is a locally asymptotical stable point if and only if the following conditions are satisfied:

$$\left.\begin{aligned} \delta_2 &> \frac{\alpha_2 \bar{u}(1-m)}{(a_2 + w_0 - \bar{w})}, \\ r &< [\delta_2 + (s + \gamma + \gamma_1 \bar{u})](a_1 + w_0 - \bar{w}), \\ \delta_1(s + \gamma + \gamma_1 \bar{u}) + \frac{r\bar{u}\ (\gamma_1 \bar{w} - d)}{(a_1 + w_0 - \bar{w})^2} &> \frac{r(s + \gamma + \gamma_1 \bar{u})}{(a_1 + w_0 - \bar{w})}. \end{aligned}\right\} \tag{7}$$

3. The Jacobian matrix at $z_3 = (u^*, v^*, w^*)$ is given as:

$$J(z_3) = \begin{bmatrix} \frac{r}{(a_1+w_0-w^*)} - \delta_1 - \alpha_1 v^*(1-m) & -\alpha_1 u^*(1-m) & \frac{ru^*}{(a_1+w_0-w^*)^2} \\ \frac{\alpha_2 v^*(1-m)}{(a_2+w_0-w^*)} & 0 & \frac{\alpha_2 u^*(1-m)v^*}{(a_2+w_0-w^*)^2} \\ d-\gamma_1 w^* & -\gamma_2 w^* & -s - \gamma - \gamma_1 u^* - \gamma_2 v^* \end{bmatrix} =$$

$$\big(a_{ij}\big)_{3\times 3} \tag{8}$$

So, the characteristic equation of $J(z_3)$ can be written as:

$$\lambda^3 + A_1\lambda^2 + A_2\lambda + A_3 = 0, \tag{9}$$

where,

$A_1 = -(a_{11} + a_{33})$, $A_2 = -(a_{13}a_{31} + a_{23}a_{32} + a_{12}a_{21} - a_{11}a_{33})$,

$A_3 = a_{11}a_{23}a_{32} + a_{12}a_{21}a_{33} - a_{13}a_{21}a_{32} - a_{12}a_{23}a_{31}$,

$\Delta = A_1A_2 - A_3 = (a_{11} + a_{33})(a_{13}a_{31} - a_{11}a_{33}) + a_{11}a_{12}a_{21} + a_{23}a_{32}a_{33} + a_{12}a_{23}a_{31} +$

$a_{13}a_{21}a_{32}$.

Now, from the Routh-Hurwitz criteria [18], z_3 is a LAS point, under the condition that $A_1 > 0, A_3 > 0$ and $\Delta > 0$.

4. Hop Bifurcation

From Theorem 2, the steady state z_3 changes as the parameter γ_2 crosses the threshold value γ_2^*, which implies that z_3 may become unstable due to Hopf bifurcation when forced to operate within particular restrictions on its parameters [19-25]. In the case where we use γ_2^* as the bifurcation parameter, the Hopf bifurcation threshold and its conditions are clearly clarified in the following theorem [].

Theorem 2. Under the following assumptions

$$A_i > 0, i = 1,2 \quad (11)$$
$$w^* > v^* \quad (12)$$
$$\gamma_2^* > 0 \quad (13)$$

where Ai's are the coefficients of the characteristic equation given in equation (9) with $\gamma_2 = \gamma_2^*$ and the formula for γ_2^* is shown in the following proof. Then, there exists a Hopf bifurcation for z_3 at $\gamma_2 = \gamma_2^*$.

Proof**:** - The value of the bifurcation parameter can be found if we set $A_1(\gamma_2^*)A_2(\gamma_2^*) - A_3(\gamma_2^*) = 0$ in equation (9). This gives:

$\gamma_2^* = \frac{(a_{11}+a_{33})(a_{13}a_{31}-a_{11}a_{33})+a_{11}a_{12}a_{21}+a_{12}a_{23}a_{31})}{(a_{23}a_{33}+a_{13}a_{21})w^*}$.

Clearly, $\gamma_2^* > 0$ if condition (13) holds. Now, at $\gamma_2 = \gamma_2^*$, equation (9) can be written as

$(\lambda + A_1)(\lambda^2 + A_2) = 0$.

According to condition (11), the above equation has three roots, a negative root $\lambda_1 = -A_1$ and two purely imaginary roots $\lambda_{2,3} = \pm i\sqrt{A_2}$. In a neighbourhood of γ_2^*, the roots have the following forms: $\lambda_1 = -A_1, \lambda_{2,3} = \rho_1(\gamma_2) \pm i\rho_2(\gamma_2)$.

Clearly, $Re(\lambda_{2,3})|_{\gamma_2=\gamma_2^*} = \rho_1(\gamma_2^*) = 0$ indicates that the first condition for Hopf bifurcation has been met at $\gamma_2 = \gamma_2^*$. Now to confirm the transversality condition, we substitute $\rho_1(\gamma_2) \pm i\rho_2(\gamma_2)$ into equation (9) and then compute its derivative with respect to d^*, $\Theta(\gamma_2^*)\psi(\gamma_2^*) + \Gamma(\gamma_2^*)\phi(\gamma_2^*) \neq 0$, where the form of $\Theta(\gamma_2^*), \psi(\gamma_2^*), \Gamma(\gamma_2^*)$ and $\phi(\gamma_2^*)$ are

$\psi(\gamma_2) = 3\rho_1^2(\gamma_2) + 2A_1(\gamma_2)\rho_1(\gamma_2) + A_2(\gamma_2) - 3\rho_2^2(\gamma_2)$,

$\phi(\gamma_2) = 6\rho_1(\gamma_2)\rho_2(\gamma_2) + 2A_1(\gamma_2)\rho_2(\gamma_2)$,

$\Theta(\gamma_2) = \rho_1^2(\gamma_2)A_1{}'(\gamma_2) + A_2{}'(\gamma_2)\rho_1(\gamma_2) + A_3{}'(\gamma_2) - A_1{}'(\gamma_2)\rho_2^2(\gamma_2)$,

$\Gamma(\gamma_2) = 2\rho_1(\gamma_2)\rho_2(\gamma_2)A_1'(\gamma_2) + A_2'(\gamma_2)\rho_2(\gamma_2)$.

Now at$\gamma_2 = \gamma_2^*$, substitution $\rho_1 = 0$ and $\rho_2 = \sqrt{A_2}$, into equation (9), the following is obtained:

$\psi(\gamma_2^*) = -2A_2(\gamma_2^*)$,

$\phi(\gamma_2^*) = 2A_1(\gamma_2^*)\sqrt{A_2(\gamma_2^*)}$,

$\Theta(\gamma_2^*) = A_3'(\gamma_2^*) - A_1'(\gamma_2^*)A_2(\gamma_2^*)$,

$\Gamma(\gamma_2^*) = A_2'(\gamma_2^*)\sqrt{A_2(\gamma_2^*)}$,

where

$A_1'(\gamma_2^*) = v^*$,

$A_2'(\gamma_2^*) = w^* - v^*,$
$A_3'(\gamma_2^*) = -2w^* - v^*.$

Hence, condition (12) gives

$$\Theta(\gamma_2^*)\psi(\gamma_2^*) + \Gamma(\gamma_2^*)\phi(\gamma_2^*) = 2A_2(\gamma_2^*)[v^* + 2w^* + 2v^*A_2(\gamma_2^*) + (w^* - v^*)2A_1(\gamma_2^*)A_2(\gamma_2^*)] \neq 0.$$

That means the Hop bifurcation has occurred at γ_2^*.

From Theorem 3, the stability condition of the stable limit cycle in $R^3_{(u,v,w)}$ is presented using the coefficient of curvature of the limit cycle. For a detailed discussion, we refer to [18].

Theorem 3 The system (1) has a stable limit cycle in $R^3_{(u,v,w)}$, if the following conditions are true:

$$\frac{r}{(a_1+w_0-u_3-w^*)^2} \neq \frac{\alpha_2(u_1+u^*)(1-m)}{(a_2+w_0-u_3-w^*)^2}. \tag{14}$$

Proof: - by shifting the $z_3 = (u^*, v^*, w^*)$ to $(0,0,0)$ by using the following transformations $u = u_1 + u^*$, $v = u_2 + v^*$, $w = u_3 + w^*$. Then the system (1) becomes:

$$\frac{du_1}{dt} = \frac{r(u_1+u^*)}{(a_1+w_0-u_3-w^*)} - \alpha_1(u_1+u^*)(u_2+v^*)(1-m) - (u_1+u^*)\delta_1$$

$$\frac{du_2}{dt} = \frac{\alpha_2(u_1+u^*)(u_2+v^*)(1-m)}{(a_2+w_0-u_3-w^*)} - \delta_2(u_2+v^*)$$

$$\frac{du_3}{dt} = s[w_0 - (u_3+w^*)] + d(u_1+u^*) - \gamma(u_3+w^*) - \gamma_1(u_1+u^*)(u_3+w^*) - \gamma_2(u_2+v^*)(u_3+w^*),$$

where the nonlinear part of the above system is presented in the following matrix is

$$\mho = \begin{pmatrix} \mho_1 \\ \mho_2 \\ \mho_3 \end{pmatrix} = \begin{pmatrix} \frac{r(u_1+u^*)}{(a_1+w_0-u_3-w^*)} - \alpha_1(1-m)u_1u_2 \\ \frac{\alpha_2(u_1+u^*)(u_2+v^*)(1-m)}{(a_2+w_0-u_3-w^*)} \\ -\gamma_1u_1u_3 - \gamma_2u_2u_3 \end{pmatrix}$$

We derive the following characteristic quantities from the nonlinear part:

$$g_{20}^0 = \frac{1}{4}\left\{\frac{\partial^2\mho_1}{\partial u_1^2} - \frac{\partial^2\mho_1}{\partial u_2^2} + 2\frac{\partial^2\mho_2}{\partial u_1\partial u_2} + i\left(\frac{\partial^2\mho_2}{\partial u_1^2} - \frac{\partial^2\mho_2}{\partial u_2^2} - 2\frac{\partial^2\mho_1}{\partial u_1\partial u_2}\right)\right\} = \frac{1}{2}\left\{\frac{\alpha_2(1-m)}{(a_2+w_0-u_3-w^*)} - \alpha_1(1-m)i\right\},$$

$$g_{11}^0 = \frac{1}{4}\left\{\frac{\partial^2\mho_1}{\partial u_1^2} + \frac{\partial^2\mho_1}{\partial u_2^2} + i\left(\frac{\partial^2\mho_2}{\partial u_1^2} + \frac{\partial^2\mho_2}{\partial u_2^2}\right)\right\} = 0,$$

$$G_{110}^0 = \frac{1}{2}\left\{\frac{\partial^2\mho_1}{\partial u_1\partial u_3} + \frac{\partial^2\mho_2}{\partial u_2\partial u_3} + i\left(\frac{\partial^2\mho_2}{\partial u_1\partial u_3} - \frac{\partial^2\mho_1}{\partial u_2\partial u_3}\right)\right\} = \frac{1}{2}\left\{\frac{r}{(a_1+w_0-u_3-w^*)^2} + \frac{\alpha_2(u_1+u^*)(1-m)}{(a_2+w_0-u_3-w^*)^2} + i\left(\frac{\alpha_2(u_2+v^*)(1-m)}{(a_2+w_0-u_3-w^*)^2}\right)\right\},$$

$$G_{101}^0 = \frac{1}{2}\left\{\frac{\partial^2\mho_1}{\partial u_1\partial u_3} - \frac{\partial^2\mho_2}{\partial u_2\partial u_3} + i\left(\frac{\partial^2\mho_2}{\partial u_1\partial u_3} + \frac{\partial^2\mho_1}{\partial u_2\partial u_3}\right)\right\} = \frac{1}{2}\left\{\frac{r}{(a_1+w_0-u_3-w^*)^2} - \frac{\alpha_2(u_1+u^*)(1-m)}{(a_2+w_0-u_3-w^*)^2} + i\left(\frac{\alpha_2(u_2+v^*)(1-m)}{(a_2+w_0-u_3-w^*)^2}\right)\right\},$$

$$W_{11}^0 = -\frac{1}{4\lambda_3(a_1(k^*)}\left(\frac{\partial^2\mho_3}{\partial u_1^2} + \frac{\partial^2\mho_3}{\partial u_2^2}\right) = 0,$$

$$W_{20}^0 = -\frac{1}{4\lambda_3(a_1(k^*)}\left(\frac{\partial^2\mho_3}{\partial u_1^2} + \frac{\partial^2\mho_3}{\partial u_2^2} - 2i\frac{\partial^2\mho_3}{\partial u_1\partial u_2}\right) = 0,$$

$$G_{21}^0 = \frac{1}{8}\left\{\frac{\partial^3 \upsilon_1}{\partial u_1^3} + \frac{\partial^3 \upsilon_1}{\partial u_1 \partial u_2^2} + \frac{\partial^3 \upsilon_2}{\partial u_2^3} + \frac{\partial^3 \upsilon_2}{\partial u_1^2 \partial u_2} + i\left(\frac{\partial^3 \upsilon_2}{\partial u_1^3} + \frac{\partial^3 \upsilon_2}{\partial u_1 \partial u_2^2} - \frac{\partial^3 \upsilon_1}{\partial u_2^3} - \frac{\partial^3 \upsilon_1}{\partial u_1^2 \partial u_2}\right)\right\} = 0,$$

Thus, the coefficient of the curvature of the limit cycle of the DOPZ system (1) is given by

$$\sigma_1^0 = Re\left\{\frac{g_{20}^0 g_{11}^0}{4} i + G_{110}^0 W_{11}^0 + \frac{G_{21}^0 + G_{101}^0 W_{20}^0}{2}\right\},$$

$$\sigma_1^0 = Re\,\frac{1}{4}\left\{\frac{r}{(a_1+w_0-u_3-w^*)^2} - \frac{\alpha_2(u_1+u^*)(1-m)}{(a_2+w_0-u_3-w^*)^2} + i\left(\frac{\alpha_2(u_2+v^*)(1-m)}{(a_2+w_0-u_3-w^*)^2}\right)\right\} = \frac{r}{(a_1+w_0-u_3-w^*)^2} - \frac{\alpha_2(u_1+u^*)(1-m)}{(a_2+w_0-u_3-w^*)^2}.$$

Thus, Condition (14) guarantees that system (1) has a stable limit cycle.

5. Numerical Simulations and Discussion

Numerical simulations support our theoretical predictions and reveal the system's numerous dynamics (1). The ode45 solver was used to find the numerical solution to our system, and all figures were made in MATLAB 2019b. We aim to study the kinetics of dissolved oxygen depletion for the phytoplankton-zooplankton interaction with the following data:

$$r = 0.35, \alpha_1 = 0.26, \alpha_2 = 0.17,\ a_1 = 0.21, a_2 = 0.21, \delta_1 = 0.11, \delta_2 = 0.11, m = 0.25, \gamma = 0.21, \gamma_1 = 0.19, \gamma_2 = 0.41, w_0 = 3, s = 2.86, d = 0.41, \quad (15)$$

To examine the effect of varying γ_2 (the consumption of oxygen by zooplankton), system (1) has been numerically solved for the data in (15) with different values. It is clear from **Figure 1** the solution converges to z_3 for $\gamma_2 > 0.22$. Further, the solution approaches a periodic behaviour for $\gamma_2 \leq 0.22$. The latter result confirms the one obtained in Theorems 2, which establishes the existence of Hopf bifurcation at $\gamma_2 = 0.22$.

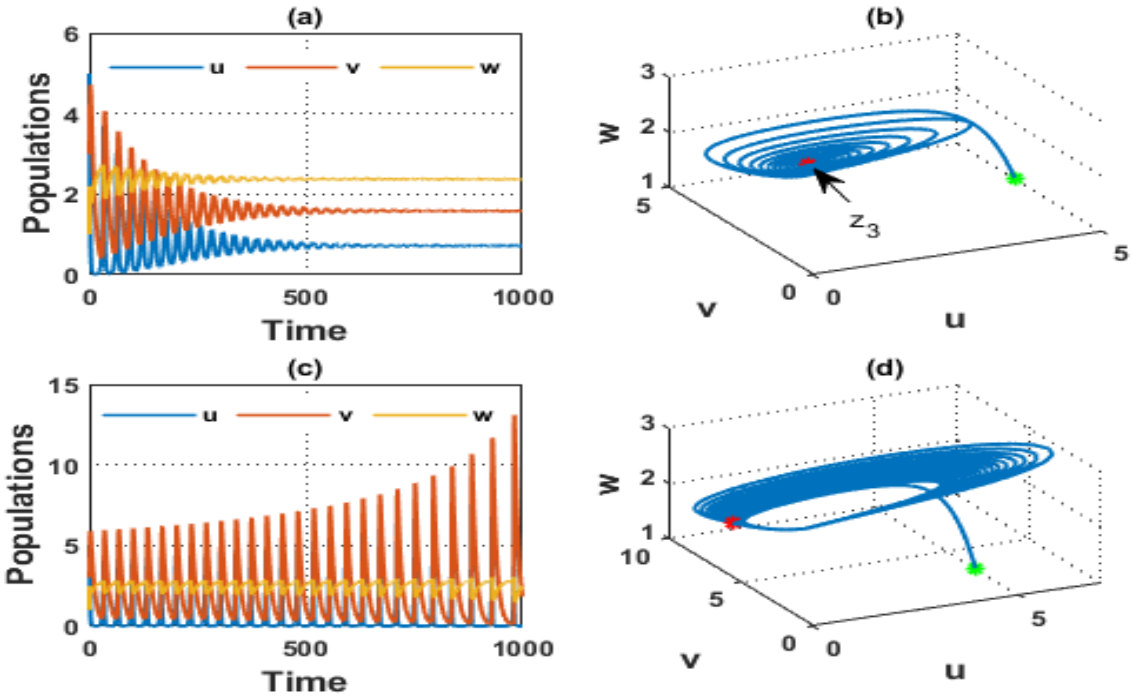

Figure 1. Dynamics of the system (1) (a) time series with $\gamma_2 = 0.41$; (b) phase portrait of (a); (c) time series with $\gamma_2 = 0.22$; (d) phase portrait of (c).

Further, **Figure 2** investigates the effect of change in the proportion of protected phytoplankton (m) on the stability properties of the system (1). It shows for $m < 0.65$, and the solution settles to the

positive equilibrium point. While for $m \geq 0.65$, the solution delivers a periodic attractor behaviour.

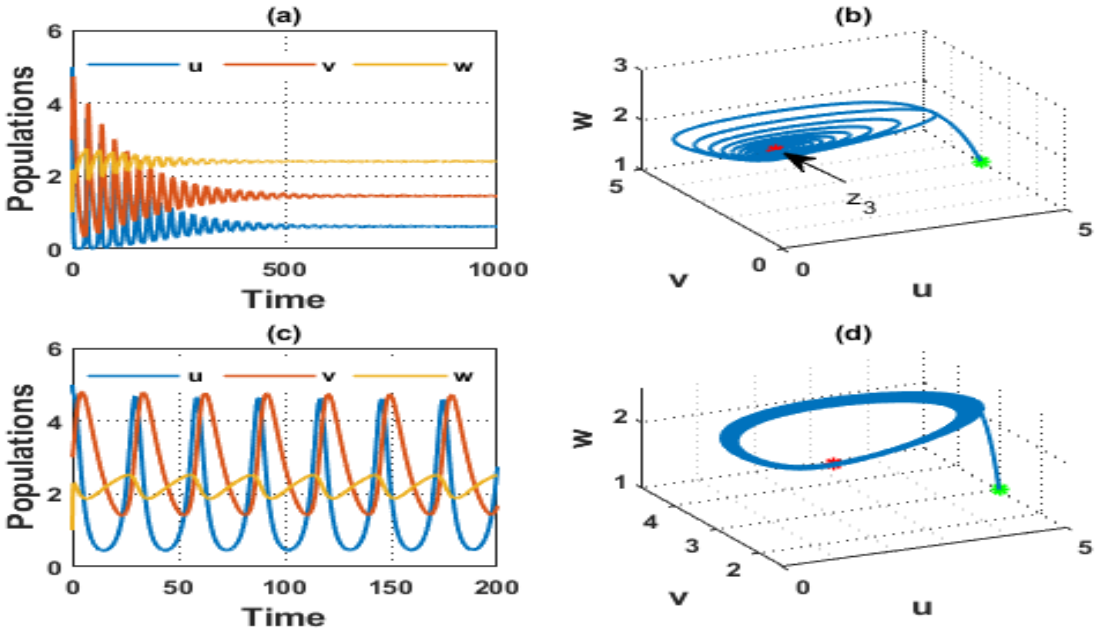

Figure 2. Dynamics of the system (1) (a) time series with $m = 0.15$; (b) phase portrait of (a); (c) time series with m = 0.65; (d) phase portrait of (c).

Further, **Figure 3** shows for different values of γ (the natural depletion rate of oxygen), the solution stabilizes at z_3 for $\gamma < 0.62$. While for $\gamma \geq 0.62$, the solution shows a periodic behaviour.

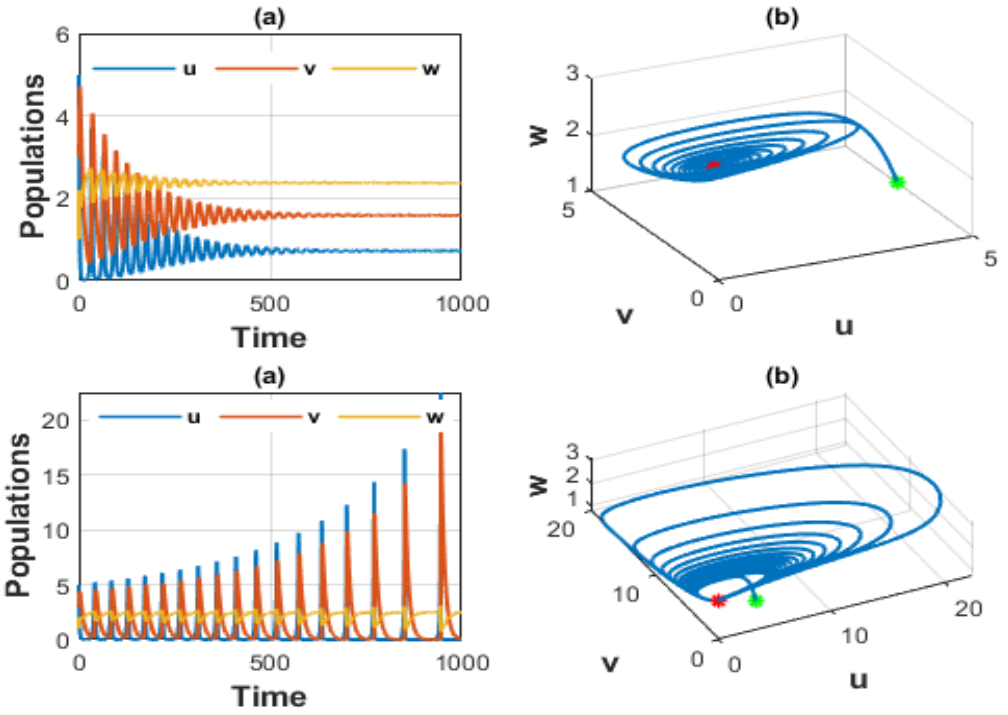

Figure 3. Dynamics of the system (1) (a) time series with $\gamma = 0.21$; (b) phase portrait of (a); (c) time series with γ = 0.62; (d) phase portrait of (c).

Further, **Figure 4** investigates the effect of change in the replenishment rate of oxygen in the marine (s) on the stability properties of the system (1). It shows for $s > 1.85$; the solution settles down to z_3. While for $s \leq 1.85$., the solution shows a periodic behaviour.

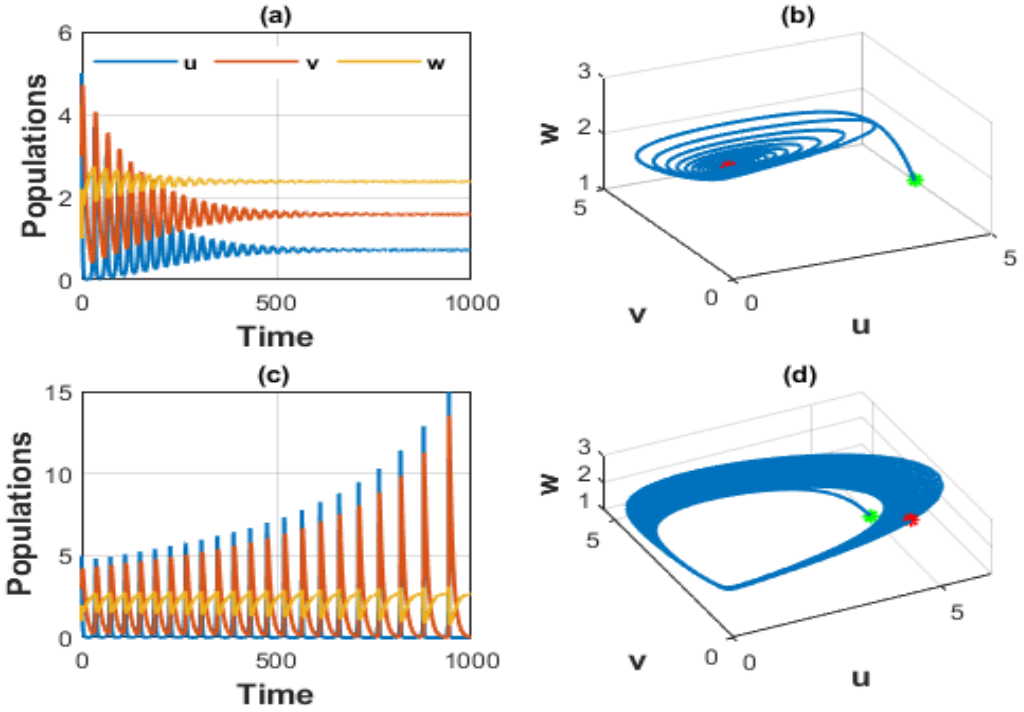

Figure 4. Dynamics of system (1) (a) time series with s=2.86; (b) phase portrait of (a); (c) time series with s=1.85; (d) phase portrait of (c); (e) time series with s=0.44; (f) phase portrait of (e).

Now the effect of changing the concentration of dissolved oxygen that comes from several sources (w_0) is explored in **Figure 5.** It shows that the solution settles asymptotically to the, z_3, for $w_0 > 2.48$. Further, the solution approaches a periodic attractor for $w_0 \leq 2.48$.

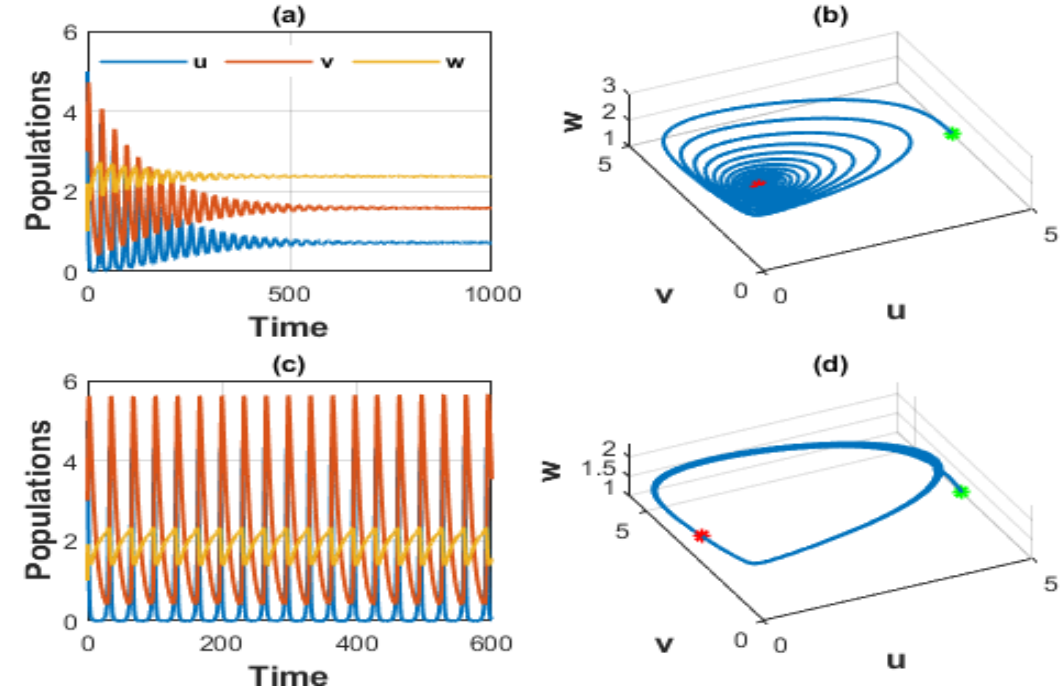

Figure 5. Dynamics of system (1) (a) time series with w_0 =3; (b) phase portrait of (a); (c) time series with $w_0 = 2.48$; (d) phase portrait of (c).

6. Conclusion

This study modified the dissolved oxygen-plankton model by considering that zooplankton feeds only on the available phytoplankton. The objective is to determine how this type of interaction

impacts the dynamics of an aquatic ecosystem. The system was analyzed theoretically and numerically. The results of the theoretical analysis revealed three stable states. Depending on the conditions, the behaviour of the three constant states was either stable or unstable. The conditions necessary for a Hopf bifurcation around the positive stable state have been identified.
Nonetheless, the numerical simulation deduced that system (1) always sways about the positive steady state when the stability criteria are met. Further, for small changing in some parameters, such that w_0, s and γ, the system (1) shows limit cycle behaviour. For future work, we suggest considering climate change's impact on the ocean's oxygen-plankton dynamics.

Acknowledgment

The authors are very grateful to the executive manager and editorial board members of the Ibn AL-Haitham Journal of Pure and Applied Sciences.

Conflict of Interest

The authors declare that they have no conflicts of interest.

Funding

There is no funding for the article.

References

1. Hull, V.; Parrella, L.; Falcucci, M. Modelling dissolved oxygen dynamics in coastal lagoons. *Ecological Modelling*, **2008**, *211*(3–4), 468–480. https://doi.org/10.1016/j.ecolmodel.2007.09.023
2. Misra, A. K. Modeling the depletion of dissolved oxygen in a lake due to submerged macrophytes. *Nonlinear Analysis: Modelling and Control*, **2010**, *15(2)*, 185–198. https://doi.org/10.15388/NA.2010.15.2.14353
3. Misra, A. K.; Chandra, P.; Raghavendra, V. Modeling the depletion of dissolved oxygen in a lake due to algal bloom: Effect of time delay. *Advances in Water Resources*, **2011**, *34*(*10*), 1232–1238. https://doi.org/10.1016/j.advwatres.2011.05.010
4. Gökçe, A. A mathematical study for chaotic dynamics of dissolved oxygen-phytoplankton interactions under environmental driving factors and time lag. *Chaos, Solitons & Fractals*, **2021**, *151*, 111268. https://doi.org/10.1016/j.chaos.2021.111268
5. Sekerci, Y.; Petrovskii, S. Mathematical modelling of plankton–oxygen dynamics under the climate change. *Bulletin of Mathematical Biology*, **2015**, *77*(*12*), 2325–2353. https://doi.org/10.1007/s11538-015-0126-0
6. Hancke, K.; Glud, R. N. Temperature effects on respiration and photosynthesis in three diatom-dominated benthic communities. *Aquatic Microbial Ecology*, **2004**, *37*(*3*), 265–281.
7. Mandal, S.; Ray, S.; Ghosh, P. B. Modeling nutrient (dissolved inorganic nitrogen) and plankton dynamics at Sagar island of Hooghly–Matla estuarine system, West Bengal, India. *Natural Resource Modeling*, **2012**, *25*(4), 629–652. https://doi.org/10.1111/j.1939-7445.2011.00116.x
8. Mondal, S.; Samanta, G.; De la Sen, M. Dynamics of Oxygen-Plankton Model with Variable Zooplankton Search Rate in Deterministic and Fluctuating Environments. *Mathematics*, **2022**, *10(10)*, 1641. https://doi.org/10.3390/math10101641
9. Turner, J.; Vollrath, F.; Hesselberg, T. Wind speed affects prey-catching behaviour in an orb web spider. *Naturwissenschaften*, **2011**, *98*, 1063–1067. https://doi.org/10.1007/s00114-011-0854-4
10. Das, A.; Samanta, G. P. Modeling the fear effect on a stochastic prey–predator system with additional food for the predator. *Journal of Physics A: Mathematical and Theoretical*, **2018**, *51*(*46*), 465601. https://doi.org/10.1088/1751-8121/aae4c6
11. Arditi, R.; Ginzburg, L. R. Coupling in predator-prey dynamics: ratio-dependence. *Journal of*

Theoretical Biology, **1989**, *139(3)*, 311–326. https://doi.org/10.1016/S0022-5193(89)80211-5

12. Sajan; Sasmal, S. K.; Dubey, B. A phytoplankton–zooplankton–fish model with chaos control: In the presence of fear effect and an additional food. *Chaos: An Interdisciplinary Journal of Nonlinear Science*, **2022**, *32(1)*, 13114. https://doi.org/10.1063/5.0069474
13. Gard, T. C.; Hallam, T. G. Persistence in food webs—I Lotka-Volterra food chains. *Bulletin of Mathematical Biology*, **1979**, *41(6)*, 877–891. https://doi.org/10.1016/S0092-8240(79)80024-5
14. Paine, R. T. Food web complexity and species diversity. *The American Naturalist*, **1966**, *100*(910), 65–75.
15. Meng, X.-Y.; Xiao, L. Stability and Bifurcation for a Delayed Diffusive Two-Zooplankton One-Phytoplankton Model with Two Different Functions. *Complexity*, **2021**, *2021*, 5560157. https://doi.org/10.1155/2021/5560157
16. Dhar, J.; Baghel, R. S. Role of dissolved oxygen on the plankton dynamics in spatio-temporal domain. *Modeling Earth Systems and Environment*, **2016**, *2(1)*, 1–15. https://doi.org/10.1007/s40808-015-0061-y
17. Hirsch, M. W.; Smale, S.; Devaney, R. L. *Differential equations, dynamical systems, and an introduction to chaos*. **2012**, Academic Press.
18. Perko, L. *Differential equations and dynamical systems* (Vol. 7). **2013**, Springer Science & Business Media.
19. LaSalle, J. P. Stability theory and invariance principles. In *Dynamical Systems*, **1976**, 211–222. Elsevier. https://doi.org/10.1016/B978-0-12-164901-2.50021-0
20. Liu, Y.; Zhao, L.; Huang, X.; Deng, H. Stability and bifurcation analysis of two species amensalism model with Michaelis–Menten type harvesting and a cover for the first species. *Advances in Difference Equations*, **2018**, *2018(1)*, 1–19. https://doi.org/10.1186/s13662-018-1752-2
21. Kuznetsov, V. A.; Makalkin, I. A.; Taylor, M. A.; Perelson, A. S. Nonlinear dynamics of immunogenic tumors: parameter estimation and global bifurcation analysis. *Bulletin of Mathematical Biology*, **1994**, *56*(*2*), 295–321. https://doi.org/10.1016/S0092-8240(05)80260-5
22. Collings, J. B. Bifurcation and stability analysis of a temperature-dependent mite predator-prey interaction model incorporating a prey refuge. *Bulletin of Mathematical Biology*, **1995**, *57(1)*, 63–76. https://doi.org/10.1007/BF02458316
23. Yu, X.; Zhu, Z.; Li, Z. Stability and bifurcation analysis of two-species competitive model with Michaelis–Menten type harvesting in the first species. *Advances in Difference Equations*, **2020**, *2020(1)*, 1–25. https://doi.org/10.1186/s13662-020-02817-4
24. Ali, N. Stability and bifurcation of a prey predator model with Qiwu's growth rate for prey. *International Journal of Mathematics and Computation*, **2016**, *27*(*2*), 30–39.
25. Jawad, S. R.; Al Nuaimi, M. Persistence and bifurcation analysis among four species interactions with the influence of competition, predation and harvesting. *Iraqi Journal of Science*, **2023**, *64(3)*, 1369–1390. https://doi.org/10.24996/ijs.2023.64.3.30
26. Mukherjee, D. Study of fear mechanism in predator-prey system in the presence of competitor for the prey. *Ecology and Genetics and Genomics*, **2020**, *15*, 100052. https://doi.org/10.1016/j.egg.2020.100052